

Unusual Specificity of a Receptor for Nd^{3+} Among Other Lanthanide Ions for Selective Colorimetric Recognition

Priyadip Das, Amrita Ghosh, and Amitava Das*

Central Salt and Marine Chemicals Research Institute (CSIR), G.B. Marg, Bhavnagar: 364002, Gujarat, India

Received February 5, 2010

A rare example of a reversible recognition of Nd^{3+} by a newly synthesized molecular receptor (L_1), having a diazo group as the reporter functionality, is reported. Studies revealed that this receptor eventually forms a $[\text{Nd}^{3+}]_2\text{L}_1$ type complex, through the formation of the intermediate complex $[\text{Nd}^{3+}]\cdot\text{L}_1$ following a two-step equilibrium process. Respective equilibrium constants for two successive processes were evaluated based on data obtained from the systematic fluorescence titration. Formation of $[\text{Nd}^{3+}]_2\text{L}_1$ caused a detectable change in color, and associated affinity constants were also evaluated from spectrophotometric titration data. A rather unusual binding mode of L_1 for Nd^{3+} ion is established by various spectroscopic studies. The remarkable specificity of L_1 for Nd^{3+} , constitutes a rare example of a highly selective receptor for this ion in the presence of excess of all other lanthanide ions.

Introduction

Cation sensing has emerged as an important area of research in the last four decades, owing to its application potential in the area of biology, clinical, and environmental studies.^{1,2} As a consequence, a large class of cation sensors, based on metal–ligand coordination, has emerged.^{1,2} However, major efforts for developing such cation sensors were focused in designing fluorescence-based sensor molecules due to their demonstrated ability to detect targeted cationic analyte present in trace/ultratrace quantities.³ In comparison, development of colorimetric sensors has received much less attention as a research area in the past. However, recent

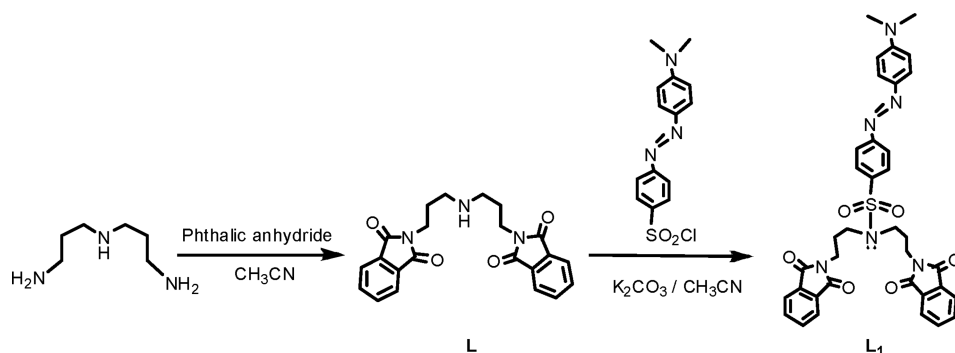
emphasis is to design colorimetric sensors that can compete with general fluorescence-based sensors in recognizing trace metal ions, owing to their ability in detecting targeted metal ion through visual detection. Among various cations, recognition and sensing of certain alkali/alkaline earth/transition-metal ions have been the focal point of the contemporary research due to their role in different cellular functions or their deleterious effects on biological systems and several other environmental concerns.⁴ In this regard, reports on the sensing and detection of different lanthanide ions are relatively scarce despite of their well-known involvement in biological/therapeutic/imaging processes and catalytic reactions.^{5,6}

The lanthanides have an ionic radius similar to that of a calcium ion, but by virtue of possessing a higher charge, they

*Corresponding author. Telephone: +91 278 2567760 [672]. Fax: +91 278 2567562/6970. Email: amitava@csmcri.org.

(1) (a) Che, Y.; Yang, X.; Zang, L. *Chem Commun.* **2008**, 1413. (b) Xue, L.; Wang, H. –H.; Wang, X. –J.; Jiang, H. *Inorg. Chem.* **2008**, 47, 4310. (c) Burdette, S. C.; Walkum, G. K.; Spingler, B.; Tsein, R. Y.; Lippard, S. J. *J. Am. Chem. Soc.* **2001**, 123, 7831. (d) Zeng, Q.; Cai, P.; Li, Z.; Qui, J.; Tang, B. Z. *Chem. Commun.* **2008**, 1094. (e) Coskun, A.; Deniz, M. Y.; Akkaya, E. U. *Org. Lett.* **2007**, 9, 607. (2) (a) Schmitt, M.; Lin, H. *Inorg. Chem.* **2007**, 46, 9139. (b) Hung, C. – H.; Chang, G. – F.; Kumar, A.; Lin, G. – F.; Luo, Li. Y.; Ching, W. – M.; Diau, E. W. – G. *Chem. Commun.* **2008**, 978. (c) Kamila, S.; John, F. C.; Mulrooney, R. C.; Middleton, M. *Tetrahedron Lett.* **2007**, 48, 7756. (3) (a) Fabbri, L.; Poggi, A. *Chem. Soc. Rev.* **1994**, 197. (b) de Silva, A. P.; Gunaratne, H. Q. N.; Gunlaugsson, T.; Huxley, A. J. M.; McCoy, C. P.; Rademacher, J. T.; Rice, T. E. *Chem. Rev.* **1997**, 97, 1515. (c) Amendola, V.; Fabbri, L.; Lincchelli, M.; Mangano, C.; Pallavicini, P.; Parodi, L.; Poggi, A. *Coord. Chem. Rev.* **1999**, 649, 190. (d) Bergonzi, R.; Fabbri, L.; Lincchelli, M.; Mangano, C. *Coord. Chem. Rev.* **1998**, 170, 31. (e) Callan, J. F.; de Silva, A. P.; Magri, D. C. *Tetrahedron* **2005**, 61, 8551. (f) Suresh, M.; Shrivastav, A.; Mishra, S.; Suresh, E.; Das, A. *Org. Lett.* **2008**, 10, 3013. (g) Suresh, M.; Ghosh, A.; Das, A. *Chem. Commun.* **2008**, 3906. (h) Valeur, B.; Leray, I. *Coord. Chem. Rev.* **2000**, 205, 3. (i) Neto, B. A. D.; Lapis, A. A. M.; Mancilha, F. S.; Vasconcelos, I. B.; Thum, C.; Basso, L. A.; Santos, D. S.; Dupont, J. *Org. Lett.* **2007**, 9, 4001. (j) Suresh, M.; Mishra, S.; Mishra, S. K.; Suresh, E.; Mandal, A. K.; Shrivastav, A.; Das, A. *Org. Lett.* **2009**, 11, 2740.

(4) (a) Atigan, S.; Ozdemir, T.; Akkaya, E. U. *Org. Lett.* **2008**, 10, 4065. (b) Dhir, A.; Valla, V.; Kumar, M. *Org. Lett.* **2008**, 4891. (c) Ko, S. K.; Yang, Y. K.; Shin, I. *J. Am. Chem. Soc.* **2006**, 128, 14150. (d) *Chemosensors of Ion and Molecule Recognition*; Desvergne, J. P., Czarnik, A. W., Eds.; Kluwer Academic Publishers: Dordrecht, The Netherlands, 1997. (e) Prodi, L.; Bolletta, F.; Montalti, M.; Zaccaroni, N. *Coord. Chem. Rev.* **2000**, 205, 59. (f) Valeur, B.; Leray, I. *Coord. Chem. Rev.* **2000**, 205, 3. (g) de Silva, A. P.; Fox, D. B.; Huxley, A. J. M.; Moody, T. S. *Coord. Chem. Rev.* **2000**, 205, 41. (5) (a) Zhang, H.; Feng, J.; Zhu, W. F.; Liu, C. Q.; Xu, S. Q.; Shao, P. P.; Wu, D. S.; Yang, W. J.; Gu, J. H. *Biol. Trace Elem. Res.* **2000**, 73, 1. (b) Salas, M.; Tuchweber, B.; Kovacs, K.; Garg, B. D. *Beitr. Pathol.* **1976**, 157, 23. (c) Nakamura, Y.; Tsumura, Y.; Tonogai, Y.; Shibata, T.; Ito, Y. *Fundam. Appl. Toxicol.* **1997**, 37, 106. (d) Liu, J. S.; Shen, Z. G.; Yang, W. D.; Che, J.; Xie, L. M.; Lei, H. Y. *J. Rare Earth* **2002**, 20, 562. (e) Xia, W. S.; Schmehl, R. H.; Li, C. J. *Tetrahedron* **2000**, 56, 7045. (6) (a) Takalo, H.; Mikkala, V. – M.; Mikola, H.; Liitti, P.; Hemmila, I. *Bioconjugate Chem.* **1994**, 5, 278. (b) Mikola, H.; Takalo, H.; Hemmila, I. *Bioconjugate Chem.* **1995**, 6, 235. (c) Mikkala, V. – M.; Helenius, M.; Hemmila, I.; Kankare, J.; Takalo, H. *Helv. Chim. Acta* **1992**, 76, 1361. (d) Mwiatkowski, M.; Samiotaki, M.; Lamminmaki, U.; Mikkala, V. – M.; Landegren, U. *Nucleic Acids Res.* **1994**, 22, 2604. (e) Werts, M. H. V.; Woudenberg, R. H.; Emmerink, P. G.; van Gassel, R.; Hofstra, J. W.; Verhoeven, J. W. *Angew. Chem., Int. Ed.* **2000**, 39, 4542. (f) Kirsch, S. F.; Liébert, C. *Eur. J. Org. Chem.* **2007**, 3711.

Scheme 1. Methodologies Adopted for Synthesis of **L** and **L₁**

generally have a higher affinity for Ca²⁺ binding sites present in biological molecules.⁷ Influences that different lanthanide ions (including Nd³⁺) have in different biological processes in living organism are reported by various researchers.^{8–10} Among different lanthanide ions, smaller trivalent metal ions are reported to be the best T-channel antagonists, and the potency for this varied inversely with ionic radii for the larger M³⁺ ions.^{8a} Lansman has shown that the strong interaction of Ln³⁺s with biologically important proteins, including ion channels and G protein-coupled receptors, occurs because these agents share biologically important properties with the divalent calcium (Ca²⁺) cation. Their similarity to Ca²⁺ with respect to ionic radii, coordination chemistry, and affinity for the oxygen-donor groups underlies their strong interaction with Ca²⁺ binding sites on a wide range of proteins.^{8b} The Ln³⁺ ions are also being used as biochemical probes to study calcium transport in mitochondria and other organelles.¹⁰ Despite such biological and therapeutic importance, selective sensing of lanthanide ions using chromogenic sensor mole-

cules has not grown as a research area as one would have expected,^{11–13} whereas reports describing the lanthanide recognition based on changes in the fluorescence as the output signal are not so uncommon.^{11,12} Among various lanthanide ions, Nd³⁺ ion is known for its biological significance as well as its application potential in laser and optoelectronics.¹⁴ Despite its vast importance, to date there is no reference available in the literature on the colorimetric detection of Nd³⁺. Moreover, the close proximity of its ionic radius with few other lanthanide ions has made the issue of designing a selective receptor for Nd³⁺ further complicated and presumably contributed to the fact that there is no report in contemporary literature on specific recognition of the Nd³⁺ ion.

In this article, we have reported a unique receptor molecule (**L₁**, Scheme 1) which could bind specifically to the Nd³⁺ ion in the presence of all other lanthanide ions present in excess. Studies revealed that on binding to the Nd³⁺, an initial enhancement in the luminescence intensity for **L₁** in Nd³⁺**L₁** was observed due to the interrupted photoinduced electron transfer (PET) process.¹⁵ Eventually, in the presence of excess Nd³⁺, [Nd³⁺]₂**L₁** was formed with a red-shifted emission maximum and a lower emission quantum yield. This was attributed to an intramolecular charge transfer (ICT) transition in [Nd³⁺]₂**L₁**. Further, a sharp change in color could be

(7) (a) Corbalan-Garcia, S.; Teruel, J. A.; Gomez-Fernandez, J. C. *Biochem. J.* **1992**, 287, 767–774. (b) Naya, M.; Cera, E. D. *Proc. Natl. Acad. Sci.* **1994**, 91, 817. (c) Wilson, J. J.; Matsushita, O.; Okabe, A.; Sakon, J. *EMBO J.* **2003**, 22, 1743. (d) Cantley, L. *Trends Neurosci.* **1986**, 9, 1. (e) Novias, A.; Vidal, J.; Franco, C.; Ribera, F.; Sener, A.; Malaisse, W. J.; Gomis, R. *Biochem. Biophys. Res. Commun.* **1997**, 231, 570.

(8) (a) Mliner, B.; Enyeart, J. J. *J. Physiol.* **1993**, 469, 639. (b) Lansman, J. B. *J. Gen. Physiol.* **1990**, 95, 679. (c) Catterall, W. A.; Perez-Reyes, E.; Snutch, T. P.; Striessnig, J. *Pharmacol. Rev.* **2005**, 57, 411. (d) Yamakage, M.; Namiki, A. *Can. J. Anaesth.* **2002**, 49, 151.

(9) (a) Enyeart, J. J.; Xu, L.; Enyeart, J. A. *Am. J. Physiol. Endocrinol. Metab.* **2002**, E1255, 282. (b) Zhang, H.; Feng, J.; Zhu, W. F.; Liu, C. Q.; Xu, S. Q.; Shao, P. P.; Wu, D. S.; Yang, W. J.; Gu, J. H. *Biol. Trace Elem. Res.* **2000**, 73, 1. (c) Salas, M.; Tuchweber, B.; Kovacs, K.; Garg, B. D. *Pathol. B.* **1976**, 157, 23. (d) Nakamura, Y.; Tsumura, Y.; Tonogai, Y.; Shibata, T.; Ito, Y. *Fundam. Appl. Toxicol.* **1997**, 37, 106. (e) Liu, J. S.; Shen, Z. G.; Yang, W. D.; Che, J.; Xie, L. M.; Lei, H. Y. *J. Rare Earth* **2002**, 20, 562.

(10) (a) Boel, E.; Brady, L.; Brzozowski, A. M.; Derewenda, Z.; Dodson, G. G.; Jensen, V. J.; Petersen, S. B.; Swift, H.; Thim, L.; Woldike, H. F. *Biochemistry* **1990**, 29, 6244. (b) Yamaguchi, M.; Isogai, M. *Mol. Cell. Biochem.* **1993**, 122, 65.

(11) (a) de Silva, A. P.; Gunaratne, H. Q. N.; Gunlaugsson, T.; Huxley, A. J. M.; McCoy, C. P.; Rademacher, J. T.; Rice, T. E. *Chem. Rev.* **1997**, 97, 1515. (b) Gunlaugsson, T.; Mac Donnell, D. A.; Parker, D. *J. Am. Chem. Soc.* **2001**, 123, 12866. (c) Parker, D.; Dickens, R. S.; Puschmann, H.; Crossland, C.; Howard, J. A. K. *Chem. Rev.* **2002**, 102, 1977. (d) Charbonnière, L. J.; Ziesler, R.; Montalti, M.; Prodi, L.; Zaccaroni, N.; Boehme, C.; Wipff, G. *J. Am. Chem. Soc.* **2002**, 124, 7779.

(12) (a) Shavaleev, N. M.; Scopelliti, R.; Gumy, F.; Bunzli, J.-C. G. *Inorg. Chem.* **2009**, 48, 2908. (b) Gunlaugsson, T.; Mac Donnell, D. A.; Parker, D. *J. Am. Chem. Soc.* **2001**, 123, 12866. (c) Yamada, T.; Shinoda, S.; Sugimoto, H.; Uenishi, J.; Tsukube, H. *Inorg. Chem.* **2003**, 42, 7932. (d) Parker, D.; Dickens, R. S.; Puschmann, H.; Crossland, C.; Howard, J. A. K. *Chem. Rev.* **2002**, 102, 1977. (e) Tsukube, H.; Shinoda, S. *Chem. Rev.* **2002**, 102, 2389. (f) Hanaoka, K.; Kikuchi, K.; Kojima, H.; Urano, Y.; Nagano, T. *J. Am. Chem. Soc.* **2004**, 126, 12470.

(13) (a) Liu, Z.; Jiang, L.; Liang, Z.; Gao, Y. *Tetrahedron* **2006**, 62, 3214. (b) Han, C.; Zhang, L.; Li, H. *Chem. Commun.* **2009**, 3545. (c) Lisowski, C. E.; Hutchison, J. E. *Anal. Chem.* **2009**, 81, 10246. (d) Zapata, F.; Caballero, A.; Espinosa, A.; Tarraga, A.; Molina, P. *Eur. J. Inorg. Chem.* **2010**, 697.

(14) (a) Waentig, L.; Roos, P. H.; Jakubowski, N. *J. Anal. At. Spectrom.* **2009**, 24, 924. (b) Lacan, T. F.; Jeandel, C. *Earth Planet. Sci. Lett.* **2005**, 232, 245. (c) Bakker, B. H.; Goes, M.; Hoebe, N.; van Ramensdonk, H. J.; Verhoeven, J. W.; Werts, M. H. V.; Hofstra, J. W. *Coord. Chem. Rev.* **2000**, 208, 3. (d) de Bettencourt-Dias, A. *Dalton Trans.* **2007**, 2229. (e) Slooff, L. H.; van Blaaderen, A.; Polman, A.; Hebbink, G. A.; Klink, S. I.; Van Veggel, F.; Reinhoudt, D. N.; Hofstra, J. W. *J. Appl. Phys.* **2002**, 91, 3955. (f) Faulkner, S.; Matthews, J. L. *Comprehensive Coordination Chemistry II*; Elsevier: Oxford, U.K., 2004; 9, 913–944. (g) Faulkner, S.; Pope, S. J. A.; Burton-Pye, B. P. *Appl. Spectrosc. Rev.* **2005**, 40, 1. (h) Beeby, A.; Dickens, R. S.; Fitzgerald, S.; Govenlock, L. J.; Maupin, C. L.; Parker, D.; Riehl, J. P.; Siligardi, G.; Williams, J. A. G. *Chem. Commun.* **2000**, 1183.

(15) (a) Suresh, M.; Das, A. *Tetrahedron Lett.* **2009**, 50, 5808. (b) Bryan, A. J.; de Silva, A. P.; de Silva, S. A.; Rupasinghe, R. A. D. D.; Sandanayake, K. R. A. S. *Biosensors* **1989**, 4, 169. (h) Bissell, R. A.; De Silva, A. P.; Gunaratne, H. Q. N.; Lynch, P. L. M.; Maguire, G. E. M.; Sandanayake, K. R. A. S. *Chem. Soc. Rev.* **1992**, 21, 187. (c) Bissell, R. A.; de Silva, A. P.; Gunaratne, H. Q. N.; Lynch, P. L. M.; Maguire, G. E. M.; McCoy, C. P.; Sandanayake, K. R. A. S. *Top. Curr. Chem.* **1993**, 168, 223. (d) He, H.; Mortellaro, M. A.; Leiner, M. J. P.; Young, S. T.; Fraatz, R. J.; Tusa, J. K. *Anal. Chem.* **2003**, 75, 549. (e) He, H.; Mortellaro, M. A.; Leiner, M. J. P.; Fraatz, R. J.; Tusa, J. K. *J. Am. Chem. Soc.* **2003**, 125, 1468. (f) Kim, J. S.; Shon, O. J.; Rim, J. A.; Kim, S. K.; Yoon, J. J. *Org. Chem.* **2002**, 67, 2348. (g) Ji, H.-F.; Brown, G. M.; Dabestani, R. *Chem. Commun.* **1999**, 609.

visually detected on formation of $[\text{Nd}^{3+}]_2\text{L}_1$, and this allows colorimetric detection of Nd^{3+} ion.

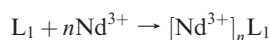
Experimental Section

Materials and Methods. Phthalic anhydride, bis(3-aminopropyl)amine-1,4'-sulfonyl chloride, 4-(dimethyl aminobenzene)azo benzene, $\text{Eu}(\text{NO}_3)_3 \cdot 5\text{H}_2\text{O}$, $\text{Er}(\text{NO}_3)_3 \cdot 5\text{H}_2\text{O}$, $\text{Yb}(\text{NO}_3)_3 \cdot 5\text{H}_2\text{O}$, $\text{La}(\text{OCOCH}_3)_3 \cdot \text{H}_2\text{O}$, $\text{Pr}(\text{NO}_3)_3 \cdot 6\text{H}_2\text{O}$, $\text{Nd}(\text{NO}_3)_3 \cdot 6\text{H}_2\text{O}$, $\text{Tb}(\text{NO}_3)_3 \cdot 5\text{H}_2\text{O}$, $\text{Ce}(\text{NO}_3)_3 \cdot 6\text{H}_2\text{O}$, $\text{Sm}(\text{NO}_3)_3 \cdot 6\text{H}_2\text{O}$, and $\text{Dy}(\text{NO}_3)_3 \cdot \text{H}_2\text{O}$ were obtained from Sigma-Aldrich and were used as received. All the other reagents used were procured from S. D Fine Chemical, India. Acetonitrile was procured from Merck, India. All solvents were dried and distilled prior to use following standard procedure.

Instrumentation. Electronic spectra were recorded using a Shimadzu UV-3101 PC or a Cary 500 Scan UV-vis-NIR spectrometer, while steady-state luminescence spectral experiments were carried out with a HORIBA JOBIN YVON spectrofluorimeter. ^1H NMR spectra were recorded on a Bruker 200 MHz, 500 MHz FT NMR (model: Avance-DPX 200) using CD_3CN as the solvent and tetramethylsilane (TMS) as an internal standard. The Fourier transform infrared spectroscopy (FTIR) spectra were recorded using Perkin-Elmer Spectra GX 2000 spectrometer.

Spectrophotometric Studies. A 1.06×10^{-4} M solution of compound L_1 (Scheme 1) in acetonitrile was prepared and stored in dark conditions. This solution was used for all spectroscopic studies after appropriate dilution. A 0.1 M solution of nitrate salt of the respective lanthanide was prepared in predried and distilled acetonitrile and each solution was stored in an inert atmosphere. For Lanthanum (La^{3+}), acetate salt was used for studies. Solution of the compound L_1 was further diluted for spectroscopic titrations, and the effective final concentration was adjusted to 2.3×10^{-5} M, while the final analyte (lanthanide ion) concentration for titration was varied from 0 to 1.39×10^{-2} M.

The equilibrium constant for the complex formation between L_1 and Nd^{3+} was evaluated using a nonlinear least-squares equation (see Supporting Information, eq 4) for the following reaction:



while the stability constant for the formation of the compound $[\text{Nd}^{3+}]_n\text{L}_1$ could be define as

$$K_n = [\text{M}_n\text{L}_1]/[\text{L}_1][\text{M}]^n \quad (1)$$

where M_nL_1 and M stands for $[\text{Nd}^{3+}]_n\text{L}_1$ and Nd^{3+} , respectively. L_1 and Nd^{3+} do not have any absorption maxima above 440 nm, so the new absorbance maxima that developed at around 508 nm on addition of Nd^{3+} to a solution of L_1 was attributed to the formation of a coordination complex $[\text{Nd}^{3+}]_n\text{L}_1$. We have selected absorbance values at these two wavelengths (A_{440} and A_{508}) for our further studies. For optical path length (l) of 1 cm, as used for the present study, the ratio A_{440}/A_{508} could be expressed by eq 2 (Supporting Information).

$$A_{440}/A_{508} = (K_n \varepsilon_{\{\text{M}_n\text{L}_1\}440} [\text{M}]^n + \varepsilon_{\{\text{L}_1\}440}) / (K_n \varepsilon_{\{\text{M}_n\text{L}_1\}508} [\text{M}]^n + \varepsilon_{\{\text{L}_1\}508}) \quad (2)$$

where $[\text{M}] = C_{\text{M}} - n[\text{M}_n\text{L}_1] = (C_{\text{M}} - nA_{440})/\varepsilon_{\{\text{M}_n\text{L}_1\}440}$ and C_{M} stands for total coconcentration of M.

The absorbance data were analyzed by using a nonlinear least-squares method and a plot of A_{440}/A_{508} vs $[\text{Nd}^{3+}]$.¹⁶ Appropriate substitution and approximation was used for evaluation of the stoichiometry and affinity constant (n and K_n , respectively).

Luminescence Titration. The standard solutions used for spectrophotometric titrations were also used for luminescence titration studies. For all measurements, $\lambda_{\text{ext}} = 508$ nm was used as an excitation wavelength. All titration experiments were performed using 2.3×10^{-5} M solutions (air equilibrated) of L_1 (in predried and distilled acetonitrile) as the final and effective concentration, while final concentrations for lanthanide ions were varied between 0 to 12.02×10^{-3} M. The binding constant for each consecutive processes was calculated from changes in fluorescence intensity with varying $[\text{Nd}^{3+}]$ using nonlinear least-squares fitting (eqs 3 and 4 for 1:1 $[\text{Nd}^{3+}] \cdot \text{L}_1$ and 1:2 $[\text{Nd}^{3+}]_2 \cdot \text{L}_1$, respectively, complex formation equilibrium, see also Supporting Information).¹⁷

$$\frac{F_c}{F_0} = 1 + \left(\frac{F_1}{F_0} - 1 \right) \left(\frac{K_1 [\text{Nd}^{3+}]}{1 + K_1 [\text{Nd}^{3+}]} \right) \quad (3)$$

K_1 and K_2 in eqs 3 and 4 correspond to respective binding constants for 1:1 and 1:2 complex formations. For eq 3, F_0 and F_1 are the fluorescence intensities at 550 nm for the free receptor and the 1:1 ($[\text{Nd}^{3+}] \cdot \text{L}_1$) complex, respectively. F_c is the fluorescence intensity for a specific $[\text{Nd}^{3+}]$, and this value is restricted for the concentration range of $(0 - 1.01 \times 10^{-3})$ M for eq 3. The concentration of the Nd^{3+} is denoted by $[\text{Nd}^{3+}]$.

For eq 4, F'_0 , F_1 , and F_2 are fluorescence intensities of the free receptor L_1 and the 1:1 ($[\text{Nd}^{3+}] \cdot \text{L}_1$) and 1:2 ($[\text{Nd}^{3+}]_2 \cdot \text{L}_1$) complexes, respectively, while F_c represents the fluorescence intensity for a specific concentration of added $[\text{Nd}^{3+}]$ to the 1:1 complex, and this value is restricted within the concentration range of $(1.01 - 12.02) \times 10^{-3}$ M.

$$\frac{F_c}{F'_0} = \frac{1 + F_1/F'_0 K_1 [\text{Nd}^{3+}] + F_1/F'_0 K_1 K_2 [\text{Nd}^{3+}]^2}{1 + K_1 [\text{Nd}^{3+}] + K_1 K_2 [\text{Nd}^{3+}]^2} \quad (4)$$

The initial enhancement in emission intensity at 550 nm was used for a tentative estimation of K_1 . Successive recalculations of K_1 were performed with eq 3 until a consistent fitting and a true value for K_1 was achieved. A similar procedure was adopted using this value of K_1 and eq 4 for the evaluation of K_2 .

Synthesis of Bis(phthalimidyl propyl)amine (L_1). Phthalic anhydride (4.74 g, 32 mmol) was added to a solution of bis(3-aminopropyl)amine (2.0 g, 15.24 mmol) in 150 mL of predried and distilled acetonitrile. The reaction mixture was stirred under reflux conditions for two days under an inert atmosphere. Then solvent was evaporated off, and 200 mL of ethanol was added to the solid residue. After stirring for 5 h, the white precipitates were filtered, collected, and dried over P_2O_5 to give the desired compound in pure form and was used for reaction without any further purification (Yield: 4.15 g; 70%). ^1H NMR (200 MHz, CDCl_3 , 25 °C, TMS); δ (ppm): 7.82–7.78 (m, 4H, ArH), 7.71–7.66 (m, 4H, ArH), 3.77 (t, $J = 6.6$ Hz, 4H, $-\text{CH}_2$), 2.78 (t, $J = 7.0$ Hz, 4H, $-\text{CH}_2$), 1.99–1.92 (m, 4H, $-\text{CH}_2$). IR (KBr): $\nu_{\text{max}}/\text{cm}^{-1} = 3461, 3031, 2936, 2816, 1771, 1711, 1640, 1398, 1364, 1044, 719, 530$. ESI-MS (M^+/z): 392.16 $[\text{M} + \text{H}]^+$ (90%). Elemental analysis $\text{C}_{22}\text{H}_{21}\text{N}_3\text{O}_4$ (391.15): calcd C, 61.51; H, 5.41; N, 10.74; found C, 61.6; H, 5.3; N, 10.7.

Synthesis of L_1 . Bis(phthalimidyl propyl) amine (L_1 ; 0.5 g, 1.278 mmol) and K_2CO_3 (0.265 g; 1.917 mmol) were added in 100 mL dry acetonitrile. The reaction mixture was refluxed for 2 h under inert atmosphere, and then acetonitrile solution of 4-(dimethylamino)phenyl diazenyl benzene-1-sulfonyl chloride

(17) (a) Alfonso, I.; Isabel Burguete, M.; Galindo, F.; Luis, S. V.; Vigarra, L. *J. Org. Chem.* **2009**, *74*, 6130. (b) Wagner, B. D.; Stojanovic, N.; Day, A. I.; Blanch, R. J. *J. Phys. Chem. B* **2003**, *107*, 10741. (c) Nigam, S.; Durocher, G. *J. Phys. Chem.* **1996**, *100*, 7135. (d) Wagner, B. D.; McManus, G. *J. Anal. Biochem.* **2003**, *317*, 233. (e) Wagner, B. D.; MacDonald, P. J. *J. Photochem. Photobiol., A* **1998**, *114*, 151.

(0.516 g; 1.6 mmol dissolved in about 40 mL of dry acetonitrile) was added in a dropwise manner to the reaction mixture and refluxed for 24 h. During the course of reaction, a significant color change from red to orange was observed. Then the reaction mixture was allowed to cool to room temperature and was filtered. Solvent was removed under reduced pressure. To the resulting residue, 30 mL of double distilled water was added, and the desired compound was extracted thrice in chloroform (3×40 mL) layer. The organic phase was collected and dried over anhydrous sodium sulfate. A light-orange colored oily residue was obtained on removal of the solvent under vacuum. This was treated with *n*-hexane, and on constant stirring, an orange solid was precipitated, which was filtered and dried to give **L₁** (0.55 g; 63%) in pure form. ^1H NMR (500 MHz, CD_3CN , 25 °C, TMS): δ (ppm): 7.86 (d, $J = 9.0$ Hz, 2H; ArH), 7.79 (m, 4H, ArH), 7.77–7.6 (m, 8H, ArH), 6.83 (d, $J = 9.0$ Hz, 2H, ArH), 3.60 (t, $J = 7.0$ Hz, 4H, $-\text{CH}_2-$), 3.23 (t, $J = 7.2$ Hz, 4H, $-\text{CH}_2-$), 3.09 (s, 6H, $-\text{CH}_3$), 1.91–1.85 (m, 4H, $-\text{CH}_2-$). IR (KBr): $\nu_{\text{max}}/\text{cm}^{-1} = 3460, 3069, 2926, 1770, 1711, 1601, 1521, 1366, 1332, 1132, 712, 594$. ESI-MS (M^+/z): 679.09 ($\text{M} + \text{H}$) $^+$ (5%), 701.03 ($\text{M} + \text{Na}$) $^+$ (100%). Elemental analysis $\text{C}_{36}\text{H}_{34}\text{N}_6\text{O}_6\text{S}$ (678.23): calcd C, 63.70; H, 5.05; N, 12.38; found C, 63.8; H, 5.1; N, 12.3.

Results and Discussion

Synthesis. Intermediate ligand **L** (Scheme 1) was synthesized by reacting bis(3-aminopropyl)amine and phthalic anhydride in appropriate ratio in a reasonably good yield. Isolated compound **L** was further used for reaction with 4-(dimethylamino)phenyl diazenyl benzene-1-sulfonyl chloride synthesis for the desired compound **L₁**. This was characterized by using various analytical and spectroscopic techniques, and data thus obtained matched well

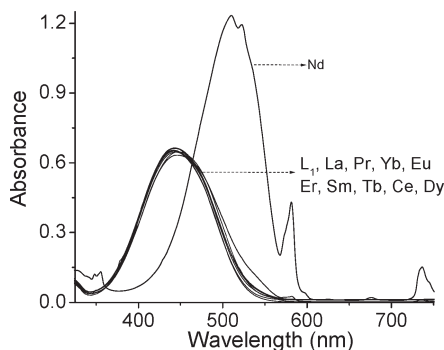
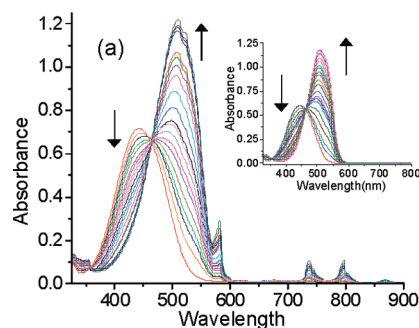


Figure 1. Absorption spectra of chemosensor (**L₁**) (2.0×10^{-5} M) in presence of different lanthanide ions ($[\text{M}^{n+}] = 8 \times 10^{-3}$ M) in CH_3CN medium.



with the formulations proposed for these two ligands. Thus, both **L** and **L₁** were isolated with desired purity and were used for further studies.

Electronic Spectroscopy. Electronic spectrum for the acetonitrile solution of **L₁** was recorded and found to have a broad absorption band at 440 nm (Figure 1), which was attributed to an intraligand charge-transfer transition band. However, a new absorption band with λ_{max} at 508 nm appeared on addition of excess Nd^{3+} . No such spectral shift was observed on addition of any other acetonitrile solutions of lanthanide ions, like La^{3+} , Pr^{3+} , Yb^{3+} , Eu^{3+} , Er^{3+} , Sm^{3+} , Tb^{3+} , Ce^{3+} and Dy^{3+} (Figure 1). Further, interference studies revealed that absorbance intensity and spectral pattern after the addition of 8.0×10^{-3} M of Nd^{3+} ion remained unchanged even in presence of large excess (0.4 M) of other lanthanide ions (Supporting Information).

However, no detectable change in electronic spectra do not completely rule out the possibility of a very weak or insignificant binding of either of these lanthanide ions to the **L₁**, as such binding may not induce sufficient perturbation in the energy of the frontier molecular orbitals to affect the HOMO–LUMO energy gap and thereby the electronic spectra.

A systematic spectrophotometric titration with varying $[\text{Nd}^{3+}]$ is shown in Figure 2a. Increase in intensity of the absorbance band at 800, 736, and 581 nm with increasing $[\text{Nd}^{3+}]$ was solely due to the absorption of the Nd^{3+} ion itself. Thus, these peaks were not observed when spectrophotometric titrations were carried out after appropriate correction for the $[\text{Nd}^{3+}]$ for each individual spectra recorded during the titration (Figure 2a inset). Further, color of the solution of **L₁** turned intense red on addition of excess Nd^{3+} , while no such color change could be detected in naked eye when other lanthanide ions were added (Figure 2b). A closer examination of the titration shows that there was no change in absorption spectral pattern until $[\text{Nd}^{3+}]$ reaches 1.0×10^{-3} M (Figure 2a). However, on further addition of increasing amount of Nd^{3+} , a gradual spectral change was observed until $[\text{Nd}^{3+}]$ reached the limiting value of 1.2×10^{-2} M. Beyond this $[\text{Nd}^{3+}]$, no further change in spectral pattern was observed. The absorbance data were analyzed by using a nonlinear least-squares method (Figure 3) using eq 2.^{13a,16}

The analysis provided the stoichiometry for the complex formation between **L₁** and Nd^{3+} and was found to be

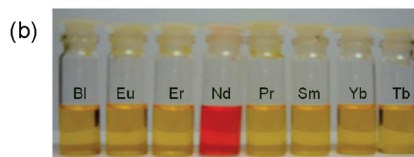


Figure 2. (a) Absorption spectra of **L₁** (2.3×10^{-5} M) in CH_3CN in presence of varying concentration of Nd^{3+} ($[\text{Nd}^{3+}] = 0\text{--}1.202 \times 10^{-2}$ M). Inset: absorption titration as shown in (a) after appropriate correction for respective $[\text{Nd}^{3+}]$. (b) Color changes observed for **L₁** (1.062×10^{-4} M) in the presence of different lanthanide ions (from left to right: **L₁**, Eu, Er, Nd, Pr, Sm, Yb, and Tb (tripositive charge of each metal ions is not shown for clarity), while $[\text{M}^{n+}] = 2.0 \times 10^{-2}$ M (M^{n+} stands for different lanthanide ions)).

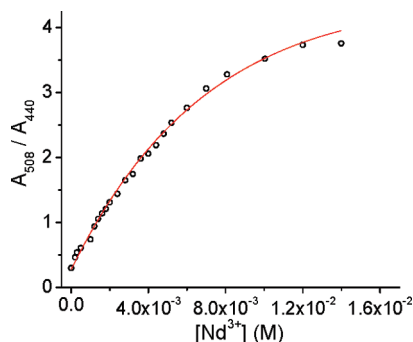


Figure 3. Variation in the ratio of absorbances A_{508}/A_{440} for a CH_3CN solution of L_1 (2.3×10^{-5} M) as a function of the varying $[\text{Nd}^{3+}]$. The solid line represents the best fit with eq 2.

1:2 with the association constant value of $(8019 \pm 425) \text{ M}^{-1}$ (correlation coefficient of 0.997).

Luminescence Spectroscopy. On excitation either at 440 or 508 nm, a very weak emission band at 550 nm could be observed in an air-equilibrated acetonitrile solution of L_1 . This weak band could be assigned as the CT in nature, while weak emission is understandable if one considers the conformational flexibility of the molecule. To ensure that any Nd^{3+} -based emission, which could arise due to the energy transfer from L_1 to Nd^{3+} , was not quenched due to the presence of the coordinated water molecule, we have recorded spectra of the Nd^{3+} ion after replacing the coordinated H_2O molecule with D_2O . For this Nd^{3+} -salt ($\text{Nd}(\text{NO}_3)_3 \cdot 5\text{H}_2\text{O}$) was dissolved in D_2O and then evaporated to dryness under an efficient vacuum system. This process was repeated four times to ascertain complete exchange of coordinated H_2O molecule with D_2O . This was then dissolved in dry and distilled acetonitrile under dinitrogen gas (to avoid any possibility of moisture getting into the solution) to prepare the standard solution. Finally emission spectra were recorded (in a cuvette fitted with a dinitrogen gas inlet and outlet tube) in presence of added L_1 (effective concentration: $[\text{L}_1] = 2.15 \times 10^{-5}$ M and $[\text{Nd}^{3+}] = (0-8.0 \times 10^{-3})$ to check whether any new emission band around at 870 nm (characteristic of the Nd^{3+} ion) appeared. However, no such new emission band could be observed. This nullifies any possibility of the ligand to metal energy transfer process and confirmed that the emission of the Nd^{3+} ion, when bound to L_1 , was not quenched due the presence of any coordinated water molecule.

Systematic studies revealed a gradual increase in luminescence intensity with an increase in $[\text{Nd}^{3+}]$, until it reached the value $\sim 1.01 \times 10^{-3}$ M (Figure 4a). However, as Nd^{3+} concentration was further enhanced from 1.01 to 12.02 mM, a steady decrease in emission intensity along with a little red-shifted emission maximum was observed (Figure 4b). Thus, the fluorescence titration tends to suggest that the observed electronic spectral changes shown in Figure 2a could be correlated to a binding phenomenon that caused the decrease in fluorescence (Figure 4b). This tends to suggest that two different equilibrium and perhaps two different complexation reactions were operational. However, this set off an obvious question, what phenomena were responsible for the fluorescence enhancement of L_1 on addition of Nd^{3+} ?

For L_1 , the amine functionality (with an unshared pair of electrons) being covalently coupled to a photoactive

signaling unit through a saturated methylene spacer, one would expect that the photoinduced electron transfer (PET) process was the dominant one for its luminescence quenching and observed lower emission quantum yield.¹⁵ This PET process gets interrupted as the lone pair of electrons on the tertiary N_{amine} atom was involved in coordination to the Nd^{3+} center. Appreciable increase in luminescence intensity for such a receptor unit, on coordination to the metal ion, without any change in band maxima is generally the main feature of such interrupted PET processes. Thus, the first set of changes, i.e., enhancement in luminescence intensity could account for the binding of the Nd^{3+} ion to the N_3 donor–receptor fragment of L_1 (A in Scheme 2).

However, one could argue in favor of the coordination to the Nd^{3+} center through the $\text{O}_{\text{C=O}}$ atoms of the two phthalimide moiety. A close comparison of the FTIR spectra recorded for L_1 and L_1 in presence of added Nd^{3+} ion only showed a nominal shift from 1711 to 1709 cm^{-1} for the C=O stretching frequency (Supporting Information). One would have expected a more pronounced stretching frequency shift for C=O in the case of coordination through one of the two carbonyl functionalities of each phthalimide moiety, and further there was no evidence for two different (coordinated and noncoordinated) C=O stretching frequency bands in the FTIR spectra recorded in the presence of added Nd^{3+} . Thus, such a possibility for the coordination of L_1 to Nd^{3+} ion through $\text{O}_{\text{C=O}}$ is not considered. Further, few earlier studies reported metal ion coordination involving the $\text{N}_{\text{phthalimide}}$ atom.¹⁸ These led us to propose a coordination through $\text{N}_{\text{amine}}(\text{N}_{\text{phthalimide}})_2$ to the Nd^{3+} ion for the first equilibrium process that lead to the observed fluorescence enhancement at 550 nm, owing to the effective interruption of the PET process (Scheme 2). The increase in fluorescence intensity of L_1 was observed until $[\text{Nd}^{3+}]$ was 1.01×10^{-3} M, however beyond this, $[\text{Nd}^{3+}]$ a small red-shifted emission band (549 nm in presence of 1.01×10^{-3} M Nd^{3+} to 553 nm in the presence of 12.02×10^{-3} M Nd^{3+}) with concomitant decrease in emission intensity was observed (Figure 4b). The dependence of the fluorescence enhancement with an increase in $[\text{Nd}^{3+}]$ ($(0-1.01) \times 10^{-3}$ M) is shown in Figure 5.

Binding constant ($K_1 = 2978 \pm 15 \text{ M}^{-1}$) could be evaluated following a nonlinear least-squares procedure (eq 3),¹⁷ where F_1/F_0 (6 ± 0.03) was the fluorescence response when no further increase in fluorescence intensity was observed on a further increase in added $[\text{Nd}^{3+}]$. This also confirmed a 1:1 binding stoichiometry. Value reported for K_1 was the average value from five independent trials. The proposed 1:1 complex formation was further confirmed by plotting the double reciprocal plot of $[1/\{(F/F_0) - 1\}]$ vs $\{1/[\text{Nd}^{3+}]\}$. Linearity of the plot (shown as inset of Figure 5) and the goodness of the fit ($r = 0.99$) confirmed the 1:1 complex ($[\text{Nd}^{3+}] \cdot \text{L}_1$) formation process (Scheme 2).

This decrease in luminescence intensity at 550 nm was observed for the $[\text{Nd}^{3+}]$ of 1.01 to 12.02 mM. Thus, this specific response seems to be for the same binding process which was responsible for the observed electronic spectral

(18) (a) Lingappa, Y.; Rao, S.; Ravikumar, S. R. V. S. S. N.; Rao, P. A. *Radiat. Eff. Defects Solids* **2007**, 162, 11. (b) Narain, G.; Klay, P. *Aust. J. Chem.* **1967**, 20, 227.

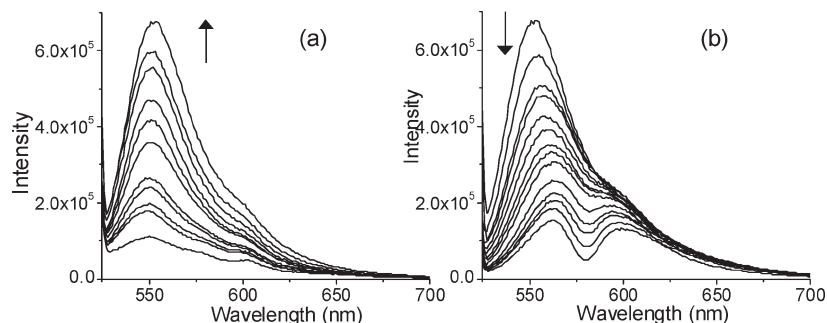
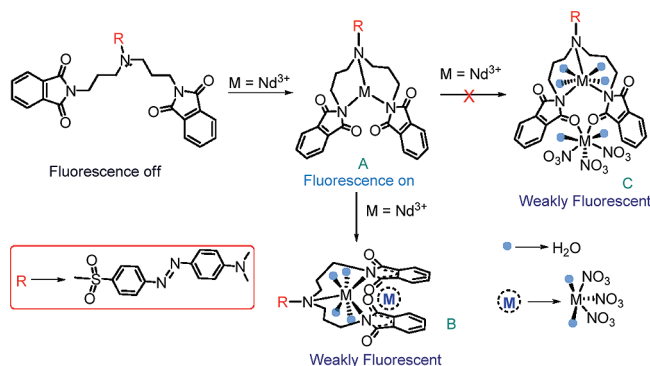


Figure 4. Changes in fluorescence spectral pattern of L_1 (2.3×10^{-5} M) in presence for varying (a) $[Nd^{3+}] = (0-1.01) \times 10^{-3}$ M and (b) $[Nd^{3+}] = (1.01-12.02) \times 10^{-3}$ M using $\lambda_{\text{exc}} = 508$ nm.

Scheme 2. Probable Modes of Coordination for L_1 to Nd^{3+} ion



changes (Figure 2a). Assuming a 1:2 complex formation with respect to Nd^{3+} , i.e., $[Nd^{3+}]_2 \cdot L_1$, the binding constant associated with this equilibrium process was further evaluated from the eq 4, where F_1 is the fluorescence intensity of the 1:1 receptor–analyte complex ($[Nd^{3+}] \cdot L_1$) at 556 nm, at the beginning of the titration, and F_2 is the intensity of the 1:2 complex ($[Nd^{3+}]_2 \cdot L_1$) at 556 nm, respectively. A good fit ($r = 0.99$) for the F_c/F_0 vs $[Nd^{3+}]$ plot further confirmed 1:2 complex formation. This was also confirmed by the nonlinear nature of the double reciprocal plot shown in the inset of Figure 6. Association constant (K_2) for this process was calculated from the luminescence titration data using eq 8 of the Supporting Information and was found to be $(9667 \pm 740) M^{-1}$. This value was close to the one that was evaluated from the spectrophotometric titration ($K_a = (8019 \pm 425) M^{-1}$) data (vide infra). Appearance of a new absorption band at 508 nm and the red-shifted emission band on addition of Nd^{3+} tends to suggest the formation of an intramolecular charge-transfer complex on binding to the second Nd^{3+} ,^{3h,19} as this process is generally associated with spectral shift. Thus, the luminescence quenching process on binding to the second Nd^{3+} could be accounted to the photoinduced ICT process involving dimethylamino azobenzene as the donor functionality and the coordinated phthalimide fragment as the acceptor unit. Based on the above discussed observations, two different models could be proposed to accommodate two different equilibrium processes (Scheme 2). According to the first model, a second Nd^{3+} is bound to $Nd^{3+} \cdot L_1$ (C in Scheme 2) involving one of the two $O_{C=O}$ atoms of each

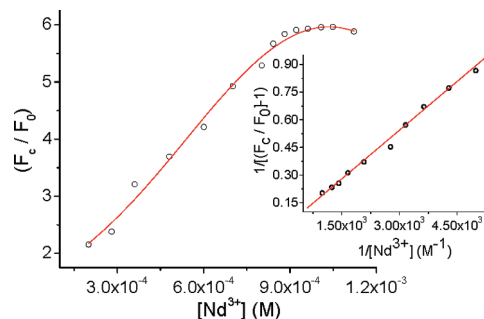


Figure 5. Fluorescence response ratio, F_c/F_0 for acetonitrile solution of L_1 as a function of varying $[Nd^{3+}]$ ($(0-1.01) \times 10^{-3}$ M). The solid line shows the fit of the data to eq 3 with $K_1 = 2978 M^{-1}$. The inset shows the linear double reciprocal plot suggesting 1:1 complex formation.

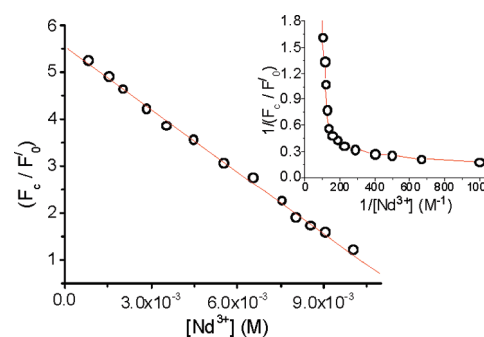


Figure 6. A plot of the variation of the ratio F_c/F_0 as a function of varying $[Nd^{3+}]$. The solid line shows the fit of the data to eq 4 with $K_1 = 2978$ and $K_2 = 9667 M^{-1}$. The inset shows the nonlinear double reciprocal plot, indicating the formation of higher-order complexes.

phthalimide moieties, while according to the alternate model (B in Scheme 2), the second Nd^{3+} ion is sandwiched between two phthalimide moieties. Absence of any evidence for two different $C=O$ stretching frequencies for the coordinated and noncoordinated $-C=O$ functionalities for L_1 in presence of large excess of Nd^{3+} led us to conclude that the second model (B in Scheme 2) was the most probable one. Possibility of the involvement of the sulphonyl ($S=O$) functionality in the $Nd^{3+}-O=S_{\text{sulphonyl}}$ type coordination could also be nullified based on the FTIR studies. FTIR spectrum for L_1 , recorded in acetonitrile solution, shows bands at 1335, 1366, and 1132 cm^{-1} , which are characteristic for the sulphonyl group. However, these characteristic bands remained almost unchanged and appeared at 1330, 1364, and 1133 cm^{-1} even after the addition of 600 mol equiv of Nd^{3+} . Thus, one would rule

(19) de Silva, A. P.; Gunaratne, H. Q. N.; Gunnlaugsson, T.; McCoy, C. P.; Maxwell, P. R. S.; Rademacher, J. T.; Rice, T. E. *Pure Appl. Chem.* **1996**, *68*, 1443.

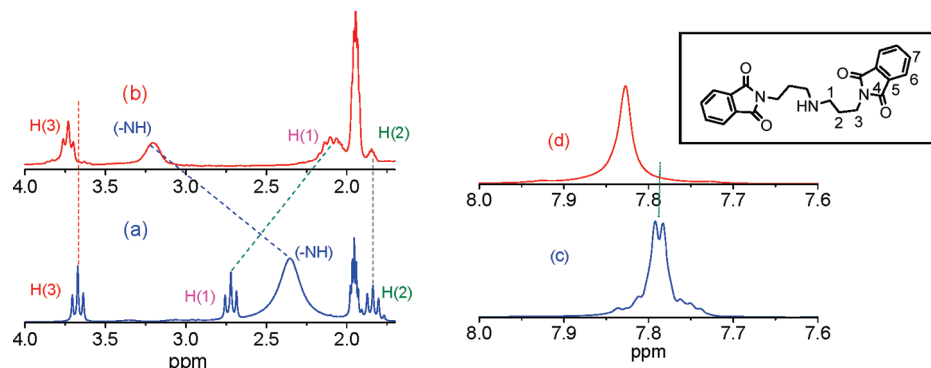


Figure 7. (a) and (c) Partial ^1H NMR (in CD_3CN) of **L** (5.1 mmol) and (b) and (d) partial ^1H NMR (in CD_3CN) of **L** in presence of added Nd^{3+} (100 equiv, 0.51 mol).

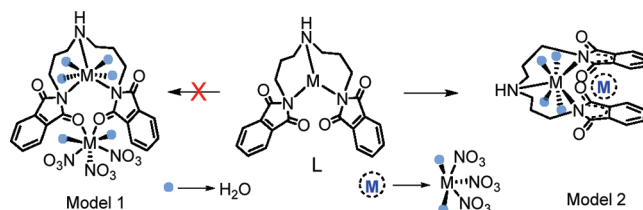
out any possibility of the involvement of sulphonyl moiety in coordination with Nd^{3+} , as for such a situation, an appreciable shift in the IR frequency for the sulphonyl functionality was expected. The proposed binding stoichiometry of 2:1 for $[\text{Nd}^{3+}]_2\text{L}_1$ and the presence of the coordinated H_2O molecules, as shown in Scheme 2, are predicted based on ES-MS spectra recorded for the solution mixture containing **L**₁ (2.3×10^{-5} M) and Nd^{3+} (12.02×10^{-3} M) in acetonitrile (Supporting Information).

^1H NMR Studies. Further confirmation of the probable binding mode for the 1:2 complex could be resolved with the help of the ^1H NMR spectra in absence and presence of varying amounts of Nd^{3+} . Owing to the limited solubility of the receptor (**L**₁) in acetonitrile (the medium in which binding studies were carried out), **L** was used as the model receptor (Scheme 1). Partial ^1H NMR spectra for **L** (in CD_3CN) in absence and presence of added Nd^{3+} is shown in Figure 7. Figure 7a and c represent the partial ^1H NMR spectra of compound **L** in CD_3CN , while Figure 7b and d are the partial spectra for **L** in presence of 100 mol equiv of Nd^{3+} ion.

A closer examination reveals that there are some remarkable differences between spectrum shown as Figure 7a and b/7c and d. Signal for H(1) is found to be upfield shifted (2.72–2.1 ppm), while an appreciable downfield shift in the signal for –N(H) hydrogen (2.35–3.05 ppm) was observed. No such detectable shift for the H(2) atom, except broadening of the signal, was observed. Interestingly, a downfield shift of the signal for H(3) (3.67–3.73 ppm) could be observed for spectra recorded in the presence of excess Nd^{3+} . Primarily, these changes in spectral pattern of the free receptor (**L**) and the receptor bound to Nd^{3+} signified complex formation between the receptor (**L**) and Nd^{3+} . One would expect to see a downfield shift for the H(1) on coordination of the N_{amine} of **L** to the Nd^{3+} center.

However, the observed overall upfield shift could be attributed to the well-known paramagnetic effect induced by the bound Nd^{3+} ion.²⁰ Little broadening with almost negligible shift in the resonance signal for H(2) could also be the result of these two opposing influences; downfield shift due to the metal ion coordination and the influence of the paramagnetic Nd^{3+} which generally induces the upfield shift. $\text{N}_{\text{phthalimide}}$ is known to be a weak-coordinating atom for metal ion coordination, and thus, the longer

Scheme 3. Probable Binding Models for $[\text{Nd}^{3+}]_2 \cdot \text{L}$ Formation



Nd^{3+} –N bond distances presumably lower the deshielding effect, which accounts for the overall downfield shift for H(3) signal. For aromatic $\text{H}^{6/7}$ protons, a downfield shift was observed (Figure 7c and d). The second Nd^{3+} ion could be bound to **L** either through coordination of the oxygen of the $\text{C}=\text{O}_{\text{phthalimide}}$ functionality (model 1, Scheme 3) or the Nd^{3+} ion could form a sandwich-type complex with two phthalimide moieties through the interaction of a π -electron cloud (model 2, Scheme 3). ^1H NMR signal for aromatic hydrogens ($\text{H}^{6/7}$) in $[\text{Nd}^{3+}] \cdot \text{L}$ shows a multiplicity (Figure 7c), while these signals get downfield shifted with little broadening on binding to the second Nd^{3+} . Further, these become more symmetrical in nature like a singlet (Figure 7d). All this tends to suggest that a second Nd^{3+} forms a sandwich-type complex between the two phthalimide rings of the receptor molecule **L**. Any binding of Nd^{3+} , involving an oxygen atom of the $\text{C}=\text{O}_{\text{phthalimide}}$ functionality in $[\text{Nd}^{3+}] \cdot \text{L}$, would have made aromatic hydrogen atoms in $[\text{Nd}^{3+}]_2 \cdot \text{L}$ even more dissymmetric in nature, a situation not observed experimentally. These observations agree well with the results obtained from FTIR studies. The balance between the up- and downfield shifts of the protons in Nd^{3+} complexes is the consequence of change in the geometry of the complexes upon coordination and is often very difficult to ascertain. Thus, based on the results of the electronic, fluorescence, and FTIR studies, it can be concluded that the probable structure for $[\text{Nd}^{3+}] \cdot \text{L}_1$ and $[\text{Nd}^{3+}]_2 \cdot \text{L}_1$ could be best represented, respectively, by A and B of Scheme 2. This result was further consolidated by the results of the detailed ^1H NMR studies with the model receptor **L**.

Conclusions

Thus, in this article, we have described a unique molecular receptor that could bind selectively only to Nd^{3+} in presence of all other lanthanide ions. An unusual binding mode for the

(20) Ansari, A. A.; Irfanullah, M.; Iftikhar, K. *Spectrochim. Acta, Part A* 2007, 67, 1178.

receptor (L_1) to the Nd^{3+} was established through detailed 1H NMR studies of a related model receptor molecule L due to the limited solubility of L_1 in common organic solvents. Further, studies revealed that this receptor could also be used for the colorimetric recognition of Nd^{3+} at the parts per million (ppm) level of concentration. The only example of such a specific colorimetric receptor is known for Yb^{3+} among all other lanthanide ions,^{13b,d} while only two other nonspecific colorimetric sensors for lanthanides are known.^{13a,c}

Acknowledgment. Authors thank DST and CSIR (India) for supporting this research. A.G. thanks CSIR

for a Senior Research Fellowship. Authors acknowledge Prof. M.D. Ward, University of Sheffield, for his valuable suggestions. A.D. thanks Dr. P.K. Ghosh, Director, CSMCRI, for his encouragement.

Supporting Information Available: Interference study of L_1 with Nd^{3+} ion in the presence of different lanthanides present in excess; 1H NMR spectra of L_1 ; ^{13}C NMR spectra of L_1 ; mass spectra of L_1 ; mass spectra for the desired complex produced between L_1 and Nd^{3+} according to the probable binding model; IR spectra of L_1 in presence and absence various concentration of Nd^{3+} . This material is available free of charge via the Internet at <http://pubs.acs.org>.